Inorganic Chemistry

Article

pubs.acs.org/IC

Multiple Pathways in the Oxidation of a NADH Analogue

Na Song, Ming-Tian Zhang, Robert A. Binstead, Zhen Fang, and Thomas J. Meyer*

Department of Chemistry, University of North Carolina at Chapel Hill, Chapel Hill, North Carolina 27599-3290, United States

Supporting Information

ABSTRACT: Oxidation of the NADH analogue, *N*-benzyl-1,4-dihydronicotinamide (BNAH), by the 1e$^-$ acceptor, $[Os(dmb)_3]^{3+}$, and 2e$^-$/2H$^+$ acceptor, benzoquinone (Q), has been investigated in aqueous solutions over extended pH and buffer concentration ranges by application of a double-mixing stopped-flow technique in order to explore the redox pathways available to this important redox cofactor. Our results indicate that oxidation by quinone is dominated by hydride transfer, and a pathway appears with added acids involving concerted hydride-proton transfer (HPT) in which synchronous transfer of hydride to one O-atom at Q and proton transfer to the second occurs driven by the formation of the stable H_2Q product. Oxidation by $[Os(dmb)_3]^{3+}$ occurs by outer-sphere electron transfer including a pathway involving ion-pair preassociation of HPO_4^{2-} with the complex that may also involve a concerted proton transfer.

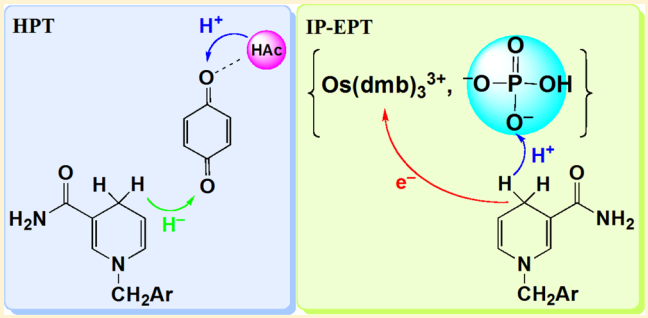

INTRODUCTION

The NAD$^+$/NADH couple is a ubiquitous redox mediator/redox cofactor in biology, distinctive for its proton-coupled electron transfer (PCET) reactivity based on C−H bond cleavage/formation reactions[1−5] with NADH providing C−H-based hydride equivalents. NADH is regenerated from NAD$^+$ by 2e$^-$/1H$^+$ PCET reduction.[6] The origin of its PCET behavior and electron transfer dynamics at the microscopic level have been explored,[2,6−11] but the involvement and interplay of key elementary steps—electron transfer (ET), proton transfer (PT), concerted electron−proton transfer (EPT), multiple site electron proton transfer (MS-EPT), hydrogen atom transfer (HAT), and hydride transfer—have yet to be fully elucidated.

For the O−H-based quinone/hydroquinone couple and redox cofactor, Q/H_2Q, seven discrete redox interconversion pathways have been identified.[12] Mechanistic complexity arises from utilization of EPT pathways as a way to avoid high-energy intermediates. A related mechanistic roadblock exists for C−H oxidation of NADH where E° = 0.93 V vs NHE for 1e$^-$ oxidation to NADH$^{\bullet+}$ and E° = 0.72 V for oxidation to NAD$^\bullet$, while $E^{\circ\prime}$ = −0.11 V for hydride transfer. These data are summarized in potential pK_a diagrams (b) and (c) in Figure 1.

There is extensive literature on oxidation of NADH and its analogues.[13−20] Most of the results are reported in organic solvents or water−organic solvent mixtures.[14,21−24] Kinetic studies under these conditions are complicated by acid-catalyzed hydrolysis reactions.[25−28] The rate of decomposition is greatly increased with added buffers, which greatly complicates the acquisition of detailed kinetic and mechanistic information.[27]

We report here the oxidation of the truncated NADH analogue, *N*-benzyl-1,4-dihydronicotinamide (BNAH, the structure is shown in Figure 1a), in water by use of a double-mixing stopped-flow spectrophotometer under conditions in which the NADH model is stable. As shown in Figure 1b and c, NADH and BNAH have closely related redox potentials and acid−base properties. The goal of the study was to explore the redox pathways utilized by this important redox cofactor toward both the 1e$^-$ outer-sphere electron oxidant $[Os(dmb)_3]^{3+}$ (dmb is 4,4′-dimethyl-2,2′-bipyridine) and the 2e$^-$/2H$^+$ acceptor benzoquinone (Q) and to assess possible roles for concerted and sequential pathways in the interconversion between BNAH and BNA$^+$.

EXPERIMENTAL SECTION

Materials. All commercial chemical reagents were used as received except as noted. All solutions were protected from light and freshly prepared with deionized water provided by a Millipore purification system (Milli-Q Synthesis A10) and purged with argon gas prior to the reactions.

Tris(4,4′-dimethyl-bipyridine) osmium(II) dichloride ($Os(dmb)_3^{2+}$) was prepared by a modified literature procedure.[31] Stock solutions of $Os(dmb)_3^{2+}$ were prepared in 0.01 M HCl and converted into $Os(dmb)_3^{3+}$ *in situ* by bubbling chlorine gas through the $Os(dmb)_3^{2+}$ solution, followed by purging with argon to remove the excess of Cl_2.

BNAH and d^2-BNAH were synthesized according to literature procedures.[32] BNAH and d^2-BNAH stock solutions were prepared with anhydrous acetonitrile (Acros Organics) and diluted into pH 9 unbuffered aqueous solutions in a glovebag for use in the kinetic studies. The total percentage of acetonitrile in reaction mixtures for kinetic studies was less than 0.5% v/v. 1,4-Benzoquinone (Q) was sublimed before use.

Received: January 10, 2014
Published: April 9, 2014

   dx.doi.org/10.1021/ic500072e | *Inorg. Chem.* 2014, 53, 4100−4105

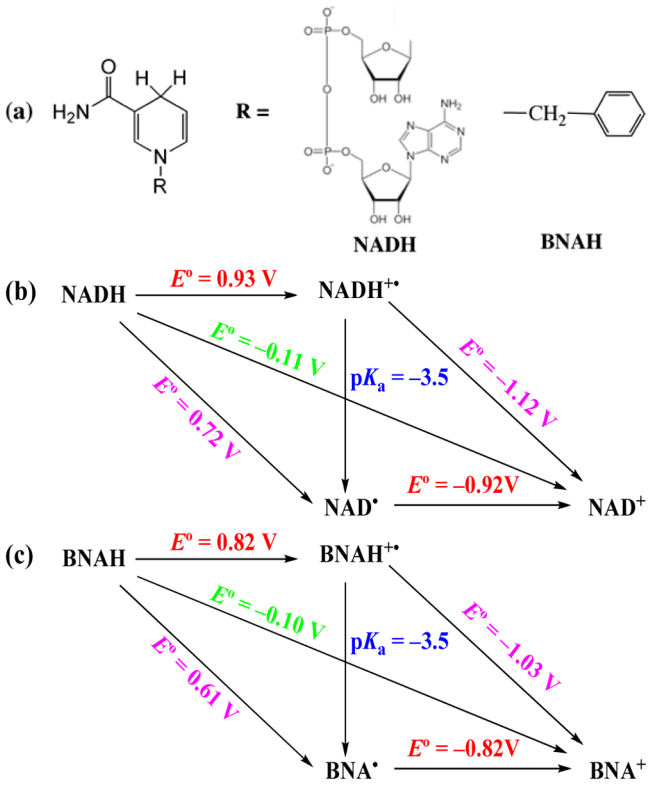

Figure 1. (a) Structures of dihydronicotinamide adenine dinucleotide (NADH) and *N*-benzyl-1,4-dihydronicotinamide (BNAH). (b) Potential $E^{\circ\prime}$(vs NHE at pH 0)−p*K*a diagram for the NAD^+/NADH couple. Diagonal lines show $1e^-/1H^+$ and $2e^-/1H^+$ PCET couples at pH 0 in water.[29] (c) Potential−p*K*a diagram for the BNA^+/BNAH couple.[30]

For kinetic studies, Os^{III} and Q reaction solutions were prepared under slightly acidic conditions, pH 4. In the double-mixing experiments, buffer solutions were mixed with the BNAH reaction solution (pH 9, unbuffered) before adding the oxidant with a delay time of 0.1 s. A total ionic strength of I = 0.8 M adjusted with NaCl was maintained in all reactions. The pK_a values of acetic acid (HAc, $pK_{a,HAc}$ = 4.42) and dihydrogen phosphate ion ($H_2OP_4^-$, $pK_{a2,H_2PO_4^-}$ = 6.44) at I = 0.8 M in water were converted from the reported values at zero ionic strength, 4.756 and 7.200,[33] respectively, by use of the Debye−Hückel equation: $\log \gamma = -0.509 z_i^2 I^{1/2}/(1 + 3.28 r I^{1/2})$ with r_{H^+} = 9 Å and $r_{Ac^-} = r_{HPO_4^{2-}}$ = 4 Å.

A Fisher Scientific Accumet AB15 pH meter was used to measure pH. Phosphoric acid-d_3 and acetic acid-d_4 were purchased from Cambridge Isotope Laboratories, Inc. and used in the kinetic isotope effect studies with pD = pH meter reading +0.4.[34] The $pK_{a,DAc}$ = 4.99 and $pK_{a2,\ D_2PO_4^-}$ = 7.03 and at I = 0.8 M in D_2O were converted from the reported values, 5.326 and 7.780, respectively, at infinite dilution[33] with $r_{H^+} = r_{D^+}$.

Kinetics. Kinetic studies were carried out on a HI-TECH SF-61DX2 stopped-flow spectrophotometer operated by the Kinetic Studio software (TgK Scientific, Ltd.) with either a tungsten light source for single wavelength observations or an MG-6560S diode array detector (3 ms integration time) and xenon light source for multi-wavelength analysis. The latter mode was used with an automatic shutter system (Uniblitz LS3) for time scales longer than 3 s as a precaution against any photolysis by the intense xenon light source. Reactions were completed in the double-mixing mode with a 1 cm optical path. Temperature was maintained at 20.0 ± 0.1 °C using a Thermo Haake A28 water bath and monitored via the internal sensor of the mixing unit. Kinetic analysis of diode array scans (380−700 nm) and single wavelength traces at 480 nm (for Os^{III} reduction) or 368 nm (for Q reduction) were performed with the SPECFIT/32 software (Spectrum Software Associates). BNAH concentrations were determined by UV−visible measurements based on known molar extinction coefficients ε_{358} = (7.9 ± 0.1) × 10^3 M^{-1} cm^{-1} and ε_{380} = (5.2 ± 0.1) × 10^3 M^{-1} cm^{-1}. Similarly, $[Os(dmb)_3^{2+}]$ was determined by UV−visible measurements at 480 nm with ε_{480} = (1.3 ± 0.1) × 10^4 M^{-1} cm^{-1}.

RESULTS AND DISCUSSION

In our experiments, oxidation of BNAH was investigated by stopped-flow spectrophotometry in the double mixing mode. In these experiments, buffers were mixed with BNAH solution (pH 9, unbuffered) with a lag time of 0.1 s before reacting with the oxidant. Limits of BNAH stability were investigated by control experiments as a function of pH and buffer concentration by spectrophotometric monitoring.

Oxidation by Q. The oxidation of BNAH by Q at 20.0 ± 0.1 °C and I = 0.8 M (NaCl) was monitored by observing the disappearance of BNAH at 368 nm where Q absorbs minimally. Pseudo-first-order conditions were utilized with Q in large excess. Figure 2a shows typical diode array scans. The observed

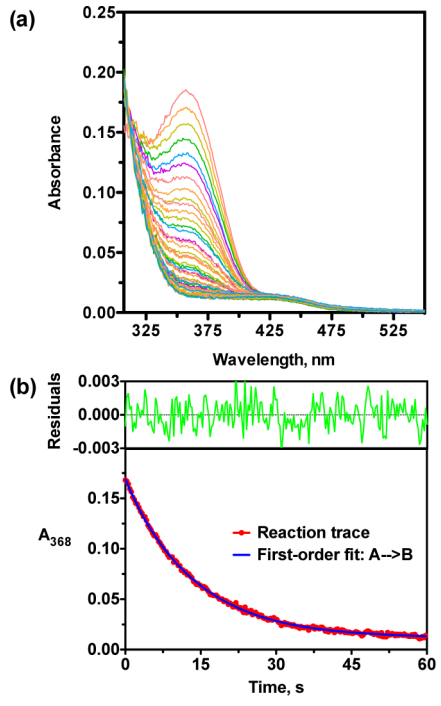

Figure 2. (a) Spectral changes accompanying oxidation of BNAH by Q. (b) Kinetic trace at 368 nm and first-order kinetic fit to the data. [BNAH] = 20 μM, $[Q]_T$ = 0.5 mM, pH 7.0, 0.01 M phosphate buffer, I = 0.8 M (NaCl), and T = 20.0 ± 0.1 °C, with monitoring over a 60 s period in the diode array mode.

rate constants were obtained from fits of absorbance−time traces at 368 nm to first-order kinetics, as shown in Figure 2b. In an initial set of experiments, the reaction was investigated by varying the concentration of Q. A linear plot of k_{obs} vs $[Q]_T$ (the total concentration of Q) was obtained as shown in Figure SI.1 of the Supporting Information. The results were consistent with the first-order rate law $-d[BNAH]/dt = k_{obs}[BNAH] = k[Q]_T[BNAH]$. From the slope of the plot, k = 159 ± 11 M^{-1} s^{-1} with a negligible intercept.

A possible acid dependence was investigated over the pH range 3.5−7.8 in 0.01 M acetate or phosphate buffer with the

dx.doi.org/10.1021/ic500072e | Inorg. Chem. 2014, 53, 4100−4105

results shown in Figure 3. A slight increase in k_{obs} was observed as the pH was decreased with the data fit to the expression,

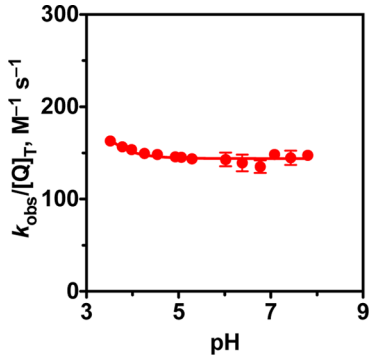

Figure 3. pH dependence in BNAH oxidation by Q. [BNAH] = 20 μM, $[Q]_T$ = 20 mM, pH 3.5−7.8, 0.01 M acetate or phosphate buffer, I = 0.8 M (NaCl), T = 20.0 ± 0.1 °C, and diode array mode.

$k_{obs}/[Q]_T = k_1 + k_2[H^+]$ with k_1 = 144 ± 1 M^{-1} s^{-1} and k_2 = (5.3 ± 0.9) × 10^4 M^{-2} s^{-1}.

The term zero-order in $[H^+]$ indicates a concerted hydride transfer pathway (note eq 1), with hydride transfer to Q giving HQ^- followed by rapid proton equilibration, eq 2. Active involvement of the C−H hydrogen is shown by a kinetic isotope effect[35] of 2.8 ± 0.1 obtained for oxidation of C−H deuterated BNAH, d^2-BNAH, in D_2O at pD 7.0. No acid or base catalysis was observed at pH/pD = 7.0 with phosphate buffer, as shown in Figure SI.2 of the Supporting Information.

$$Q + BNAH \rightarrow HQ^- + BNA^+ \quad k_1 = k_{H^-} \tag{1}$$

$$HQ^- + H^+ \rightarrow H_2Q \quad \text{rapid} \tag{2}$$

With this interpretation, $k_1 = k_{H^-}$ for the hydride transfer step. From the potential data in Figure 1c, $E^{\circ\prime}$ = −0.10 V for the BNA^+/BNAH couple and $E^{\circ\prime}$ = 0.40 V calculated for the Q/HQ^- couple[12] show that hydride transfer occurs with ΔG° = −1.0 eV (Table SI.1, Supporting Information). The detection of radical cations of $AcrH_2^{\bullet+}$[16] and $AcrHR^{\bullet+}$[36] was described in acetonitrile under acid-promoted conditions, where the driving force for electron transfer is only slightly positive (e.g., ΔG° = +0.12 eV for the latter). In our case, the hydride transfer pathway enjoys the energetic advantage of avoiding the high-energy one-electron intermediates $Q^{\bullet-}$ and $BNAH^{\bullet+}$, with ΔG° = +0.72 eV, or hydrogen atom transfer to give $HQ^\bullet$ and $BNA^\bullet$ with ΔG° = +0.27 eV (Table SI.1, Supporting Information), although the latter cannot be ruled out.

The appearance of the pathway first order in $[H^+]$ is consistent with preprotonation of Q to give HQ^+, followed by hydride transfer (eqs 3 and 4). $k_{H^-,HQ^+} = k_2 K_{a,HQ^+}$ occurs at the diffusion-controlled limit with pK_{a,HQ^+} assumed to be −6 estimated in an earlier study.[12] Although complex microscopically, the advantage of this pathway is that the final products are formed with their stable electronic and proton compositions with $\Delta G^\circ \approx -1.9$ eV for the $2e^-/1H^+$ step in eq 4.

$$Q + H^+ \leftrightharpoons HQ^+ \quad 1/K_{a,HQ^+} \tag{3}$$

$$HQ^+ + BNAH \rightarrow H_2Q + BNA^+ \quad k_2 = k_{H^-,HQ^+}/K_{a,HQ^+} \tag{4}$$

We have also found evidence for acetic acid catalysis at pH 3.5 by varying the total concentration of an acetic acid/acetate buffer at constant pH. Experimentally, the reaction rate is observed to increase with increasing acid concentration with saturation reached at [HAc] ∼ 0.4 M. This observation reveals a mechanism involving prior association between HAc and Q followed by hydride transfer from BNAH to the H-bonded adduct between Q and HAc (eqs 6 and 7). The variation in k_{obs} with [HA] is consistent with eq 5, where $K_{A,Q}$ is the equilibrium constant for the pre-equilibrium.

$$\frac{k_{obs}}{[Q]_T} = \frac{k + k_3 K_{A,Q}[HA]}{1 + K_{A,Q}[HA]} \tag{5}$$

$$Q + HAc \leftrightharpoons Q\text{---}HAc \quad K_{A,Q} \tag{6}$$

$$Q\text{---}HAc + BNAH \rightarrow H_2Q + Ac^- + BNA^+ \quad k_3 = k_{HPT} \tag{7}$$

Fitting the data at 20.0 ± 0.1 °C and I = 0.8 M (NaCl) to eq 5 (Figure 4) yields $K_{A,Q}$ = 15 ± 6 M^{-1}, k_3 = 189 ± 1 M^{-1} s^{-1}, and k = 155 ± 6 M^{-1} s^{-1} (= $k_1 + k_2[H^+]$). The latter is consistent with the appearance of the acid dependent pathway in eqs 3,4.

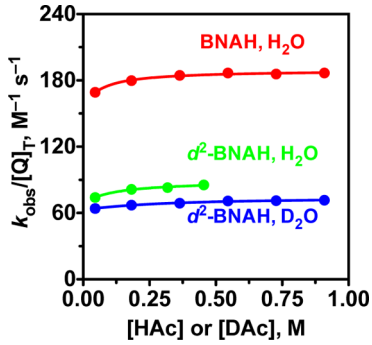

Figure 4. Oxidation of BNAH in H_2O (red): [BNAH] = 20 μM, $[Q]_T$ = 20 mM, pH 3.5, 0.05−1.00 M acetate buffer, $[HAc]/[Ac^-]$ = 10/1, I = 0.8 M (NaCl), and T = 20.0 ± 0.1 °C. Oxidation of d^2-BNAH in H_2O (green): [BNAH] = 20 μM, $[Q]_T$ = 20 mM, pH 3.5, 0.05−0.5 M acetate buffer, $[HAc]/[Ac^-]$ = 10/1, I = 0.8 M (NaCl), and T = 20.0 ± 0.1 °C. Oxidation of d^2-BNAH in D_2O (blue): [d^2-BNAH] = 20 μM, $[Q]_T$ = 20 mM, pD 4.1, $[DAc]/[Ac^-]$ = 10/1, 0.05−1.00 M acetate buffer, I = 0.8 M (NaCl), and T = 20.0 ± 0.1 °C. All error bars are smaller than the solid dots.

The kinetic study was repeated for d^2-BNAH in both H_2O (at pH 3.5, $[HAc]/[Ac^-]$ = 10/1) and D_2O (at pD 4.1, $[DAc]/[Ac^-]$ = 10/1) at I = 0.8 M (NaCl), which gave $k_3^D(H_2O)$ = 89 ± 3 M^{-1} s^{-1}, $k^D(H_2O)$ = 68 ± 4 M^{-1} s^{-1}, $K_{A,Q}^D(H_2O)$ = 8.6 ± 6.6 M^{-1}, $k_3^D(D_2O)$ = 75 ± 1 M^{-1} s^{-1}, $k^D(D_2O)$ = 62 ± 1 M^{-1} s^{-1}, and $K_{A,Q}^D(D_2O)$ = 3.2 ± 0.9 M^{-1}. The data are all summarized in Table SI.2 of the Supporting Information. Under these conditions the C−H/C−D kinetic isotope effect (KIE) for oxidation of BNAH compared to d^2-BNAH in H_2O is 2.3 ± 0.2 for k. This value includes contributions from the pathways in both eqs 1 and 4 with the former dominating and resulting in a relatively small H_2O/D_2O solvent KIE of 1.1 ± 0.1.

For the reaction in eq 7, BNAH/d^2-BNAH, KIE in H_2O was 2.1 ± 0.1, the solvent KIE for d^2-BNAH oxidation was 1.2 ± 0.1, and the total KIE was 2.5 ± 0.1. The equilibrium isotope effect for pre-equilibrium adduct formation[37] is 4.6 ± 2.3 for $K_{A,Q}$ with a combined isotope effect of, $k_3^H K_{A,Q}^H / k_3^D K_{A,Q}^D$ = 12 ± 6. These observations suggest the mechanism in eqs 6 and 7 in

dx.doi.org/10.1021/ic500072e | Inorg. Chem. 2014, 53, 4100−4105

which prior association occurs between Q and HAc followed by hydride transfer from BNAH to the adduct, Q---HAc, by concerted hydride-proton transfer (HPT)[38] with hydride transfer to one O-atom at Q and proton transfer to the other. Although also complex microscopically, this pathway benefits by forming energetically stable products in a single microscopic step. For the HPT reaction in eq 7, $\Delta G^{\circ\prime} \approx -nF[E^{\circ\prime}(Q/H_2Q) - E^{\circ\prime}(BNA^+/BNAH)] + 0.059pK_{a,HAc} \approx -1.3$ eV.

Acid catalysis of 10-methyl-9,10-dihydroacridine oxidation by benzoquinone has been observed both in 3%[39,40] and 20%[41] ethanol–water mixtures but with a different interpretation from the one given here. As noted above, our results on BNAH, obtained by the double-mixing stopped-flow technique, are free of potential complications from acid-catalyzed hydrolysis[25,26] with formation of the acridone.[17,42]

Oxidation by $[Os(dmb)_3]^{3+}$. The oxidation of BNAH by the $1e^-$ oxidant $[Os(dmb)_3]^{3+}$ was investigated at 20.0 ± 0.1 °C by monitoring the appearance of $[Os(dmb)_3]^{2+}$ at 480 nm. Stoichiometric oxidation of BNAH by $[Os(dmb)_3]^{3+}$ at a 1:2 ratio was conducted at pH 7.0 (I = 0.8 M, NaCl) with added 0.01 M phosphate buffer ($H_2PO_4^-/HPO_4^{2-}$). The results are shown in Figure 5a. The experiment was repeated with 1:1 and 2:1 ratios of BNAH to oxidant. The results of absorption spectral changes were all consistent with the expected $2e^-$ oxidation of BNAH to BNA^+ by the net reaction, $2\ [Os(dmb)_3]^{3+} + BNAH \rightarrow 2\ [Os(dmb)_3]^{2+} + BNA^+ + H^+$.

Figure 5b and c show typical kinetic traces for the appearance of $[Os(dmb)_3]^{2+}$ at 480 nm in diode array mode and single wavelength mode, respectively. The data were fit by using SPECFIT/32. There are two possible models for the observed second-order kinetics: 2{1}*A + B → C + D (for a 2:1 stoichiometry) with the second step much more rapid than the first, and A + B → C + D, where the second step is not competitive with initial consumption of $[Os(dmb)_3]^{3+}$ by the small excess of BNAH. The former model gives excellent fits for $[Os(dmb)_3]^{3+}]/[BNAH] = 2/1$ (Figure 5b), while residual errors appear for $[Os(dmb)_3]^{3+}]/[BNAH] = 1/3.5$ (Figure 5c) with a better fit to the latter model. Given the similarity in rate constants at 2/1 and 1/3.5 oxidant/reductant ratios, second-order rate constants for the reaction were obtained by fitting the data to the 2:1 stoichiometry model and the rate law in eq 8.

The pH dependence of the reaction was investigated over the range pH 6.0–7.8 with added 0.01 M phosphate buffer (at I = 0.8 M, NaCl, and 20.0 ± 0.1 °C). As shown in Figure SI.3 of the Supporting Information, there was no effect on the rate over this pH range with dilute added buffers.

$$-d[BNAH]/dt = k'[[Os(dmb)_3]^{3+}][BNAH] \quad (8)$$

$$k' = k_4 + k_5[HPO_4^{2-}] \quad (9)$$

The reaction was also investigated at higher buffer concentrations, 0.05–0.16 M, at pH 7.0 to search for a possible EPT pathway or pathways. As shown in Figure 6, the second-order rate constant for BNAH oxidation under these conditions with added $[HPO_4^{2-}]$ is consistent with eq 9 with $k_4 = (2.1 \pm 0.1) \times 10^5\ M^{-1}\ s^{-1}$ and $k_5 = (8.2 \pm 0.4) \times 10^5\ M^{-2}\ s^{-1}$, respectively. The same experiments were repeated for oxidation of d^2-BNAH in D_2O as a function of added DPO_4^{2-}. Under these conditions, k_{obs} increased linearly with $[DPO_4^{2-}]$. Analysis of the data gave $k_4^D = (1.4 \pm 0.1) \times 10^5\ M^{-1}\ s^{-1}$ and $k_5^D = (4.5 \pm 0.3) \times 10^5\ M^{-2}\ s^{-1}$ yielding KIEs of 1.5 ± 0.1 for k_4 and 1.8 ± 0.1 for k_5.

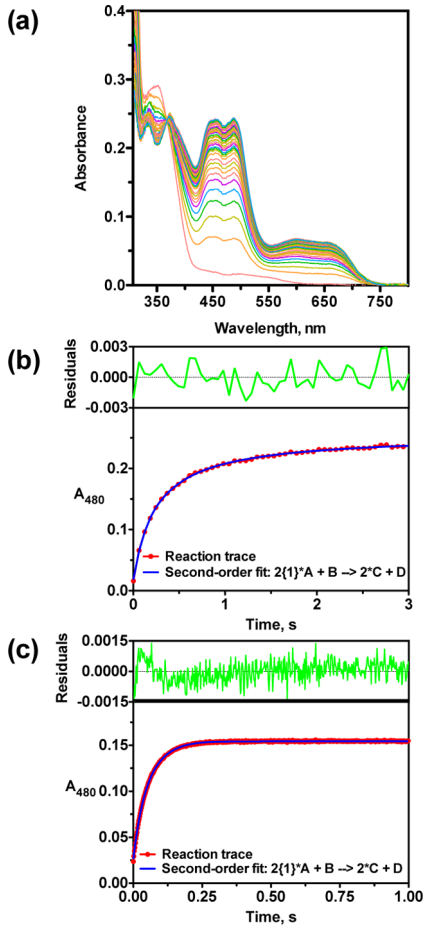

Figure 5. (a) Spectral changes for BNAH oxidation by $Os^{III}(dmb)_3$. [BNAH] = 10 μM, $[Os^{III}(dmb)_3]$ = 20 μM, pH 7.0, 0.01 M phosphate buffer, I = 0.8 M (NaCl), T = 20.0 ± 0.1 °C, over 3s, and diode array mode. (b) Kinetic trace at 480 nm and a second-order kinetic fit to the data in (a). (c) Kinetic trace at 480 nm and second-order fit. [BNAH] = 42 μM, $[Os^{III}(dmb)_3]$ = 12 μM, pH 7, 0.05 M phosphate buffer, I = 0.8 M (NaCl), T = 20.0 ± 0.1 °C, and single wavelength mode.

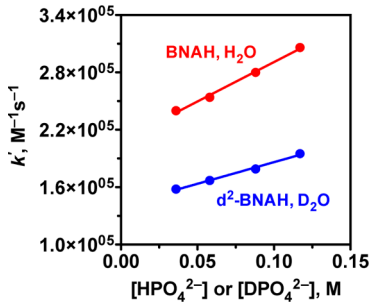

Figure 6. Oxidation of BNAH in H_2O (red): [BNAH] = 42 μM, $[Os^{III}(dmb)_3]$ = 12 μM, pH 7.0, 0.05–0.16 M phosphate buffer, I = 0.8 M (NaCl), and T = 20.0 ± 0.1 °C. Oxidation of d^2-BNAH in D_2O (blue): [d^2-BNAH] = 37 μM, $[Os^{III}(dmb)_3]$ = 11 μM, pD 7.6, 0.05–0.16 M phosphate buffer, I = 0.8 M (NaCl), T = 20.0 ± 0.1 °C, and single wavelength mode. All error bars are smaller than the solid dots.

In the rate expression in eq 9, the term zero-order in $[H^+]$ and $[HPO_4^{2-}]$ is consistent with rate-limiting outer-sphere electron transfer oxidation of BNAH (eq 10), followed by rapid proton loss and further oxidation. Rate-limiting electron

dx.doi.org/10.1021/ic500072e | Inorg. Chem. 2014, 53, 4100–4105

transfer is consistent with the relatively small k_H/k_D KIE and is not inhibited by $[Os(dmb)_3]^{3+}$ due to the fast deprotonation of $BNAH^{\bullet+}$.[43] The origin of the term in the rate law first order in $[HPO_4^{2-}]$ is less obvious. An analogous term appears in the rate law for oxidation of H_2Q to Q by $[Os(dmb)_3]^{3+}$ with added Ac^- anion.[12] It was attributed to concerted multiple site electron proton transfer (MS-EPT) with preassociation with Ac^- followed by electron transfer to the complex and proton transfer to the base (eq 13), which occurred with a H/D KIE of 2.6 ± 0.1. A similar mechanism for oxidation of BNAH with the ion-paired base acting as a proton acceptor may also occur (eqs 14 and 15), as suggested by the KIE of 1.8 ± 0.1 for k_5. The driving force for a MS-EPT reaction is favorable with $\Delta G^{\circ\prime} \approx -nF[E^{\circ\prime}(Os^{III/II}) - E^{\circ\prime}(BNA^{\bullet}/BNAH)] - 0.059pK_{a2,H_2PO_4^-} \approx -0.40$ eV.

$$[Os(dmb)_3]^{3+} + BNAH \rightarrow [Os(dmb)_3]^{2+} + BNAH^{\bullet+} \quad k_4 = k_{et} \tag{10}$$

$$BNAH^{\bullet+} \leftrightharpoons BNA^{\bullet} + H^+ \quad K_{a,BNAH^{\bullet+}} \tag{11}$$

$$[Os(dmb)_3]^{3+} + BNA^{\bullet} \rightarrow [Os(dmb)_3]^{2+} + BNA^+ \quad \text{rapid} \tag{12}$$

$$[Os(dmb)_3]^{3+} + H\text{-}Q\text{-}H\text{---}Ac^- \rightarrow [Os(dmb)_3]^{2+} + HQ^{\bullet} + HAc \tag{13}$$

$$[Os(dmb)_3]^{3+} + HPO_4^{2-} \leftrightharpoons \{[Os(dmb)_3]^{3+}, HPO_4^{2-}\}\ K_{IP} \tag{14}$$

$$\{[Os(dmb)_3]^{3+}, HPO_4^{2-}\} + BNAH \rightarrow [Os(dmb)_3]^{2+} + H_2PO_4^- + BNA^{\bullet} \quad k_5 = K_{IP}k_{EPT,IP} \tag{15}$$

CONCLUSIONS

As found in an earlier study on $1e^-$ interconversion between quinone and hydroquinone, oxidation of BNAH to BNA^+, as a surrogate for the NAD^+/NADH couple, occurs by multiple pathways. A summary is given in Scheme 1. With Q as the oxidant, both $1e^-$ and $2e^-$ pathways are accessible, but reactivity may be dominated by hydride transfer that has the energetic advantage of avoiding the high-energy $1e^-$ intermediates, $BNAH^{\bullet+}$ and $BNA^{\bullet}$. Proton content also plays a role, as in the quinone/hydroquinone couple, as shown by the appearance of pathways for general acid catalysis and specific acid catalysis with HAc. Prior protonation of Q to give HQ^+, although thermodynamically unfavorable, has the advantage of forming the final products in their equilibrium proton compositions in the hydride transfer step that follows. Similarly, in the proposed HPT reaction with added HAc, synchronous transfer of hydride to Q at one O-atom may occur in concert with proton transfer to the other to give the stable H_2Q product.

With $[Os(dmb)_3]^{3+}$ as the oxidant, and only $1e^-$ pathway accessible, as shown in Scheme 2, the reaction is dominated by initial $1e^-$ oxidation to $BNAH^{\bullet+}$. Initial oxidation is followed by proton loss and a second oxidation step. Appearance of a pathway first order in added $[HPO_4^{2-}]$ may arise from initial ion-pairing with the cationic oxidant and the ion-paired base assisting with oxidation of the C−H bond.

There are significant differences in behavior between the redox interconversions between BNAH and BNA^+ and Q and H_2Q. They arise from energetic access in the Q/H_2Q couple to $1e^-$ pathways based on accessible semiquinone intermediates. For BNAH, the redox chemistry based on the C−H bond is dominated by hydride transfer that avoids relatively high-energy $1e^-$ intermediates. Base effects do not play a role due to the inability of the C−H bond to undergo significant H-bonding.

Scheme 1. Pathways for Oxidation of BNAH by Quinone

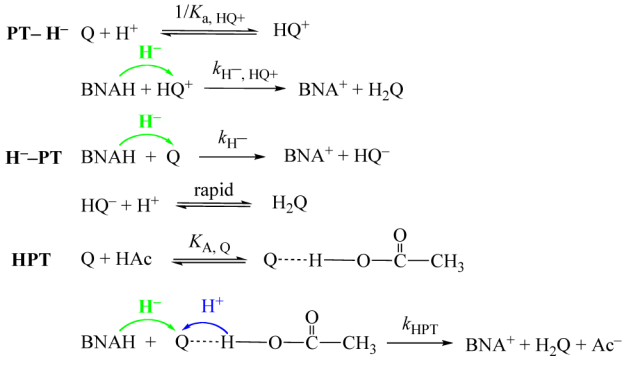

Scheme 2. Pathways for Oxidation of BNAH by $[Os(dmb)_3]^{3+}$

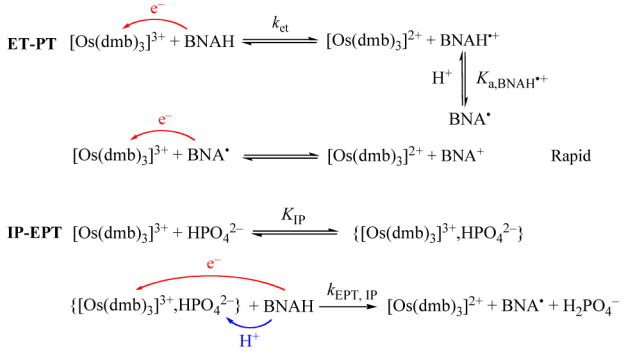

ASSOCIATED CONTENT

Supporting Information

Experimental details and data analysis. This material is available free of charge via the Internet at http://pubs.acs.org.

AUTHOR INFORMATION

Corresponding Author

*E-mail: tjmeyer@email.unc.edu.

Notes

The authors declare no competing financial interest.

ACKNOWLEDGMENTS

This work was supported by the National Science Foundation under Grant CHE-0957215, supporting N.S. and M.-T.Z. We acknowledge support from the UNC EFRC, Center for Solar Fuels, an Energy Frontier Research Center funded by the U.S. Department of Energy, Office of Science, Office of Basic Energy Sciences, under Award Number DE-SC0001011, supporting R.A.B. and Z.F.

REFERENCES

(1) Rodkey, F. L. *J. Biol. Chem.* **1955**, *213*, 777.

(2) Warren, J. J.; Tronic, T. A.; Mayer, J. M. *Chem. Rev.* **2010**, *110*, 6961.
(3) Fromme, P. *Photosynthetic Protein Complexes: A Structural Approach*; Wiley-VCH: Weinheim, Germany, 2008.
(4) Aliverti, A.; Pandini, V.; Pennati, A.; de Rosa, M.; Zanetti, G. *Arch. Biochem. Biophys.* **2008**, *474*, 283.
(5) Medina, M. *FEBS J.* **2009**, *276*, 3942.
(6) Weinberg, D. R.; Gagliardi, C. J.; Hull, J. F.; Murphy, C. F.; Kent, C. A.; Westlake, B. C.; Paul, A.; Ess, D. H.; McCafferty, D. G.; Meyer, T. J. *Chem. Rev.* **2012**, *112*, 4016.
(7) Huynh, M. H. V.; Meyer, T. J. *Chem. Rev.* **2007**, *107*, 5004.
(8) Dempsey, J. L.; Winkler, J. R.; Gray, H. B. *Chem. Rev.* **2010**, *110*, 7024.
(9) Costentin, C. *Chem. Rev.* **2008**, *108*, 2145.
(10) Hammes-Schiffer, S.; Stuchebrukhov, A. A. *Chem. Rev.* **2010**, *110*, 6939.
(11) Zhang, M. T.; Irebo, T.; Johansson, O.; Hammarström, L. *J. Am. Chem. Soc.* **2011**, *133*, 13224.
(12) Song, N.; Gagliardi, C. J.; Binstead, R. A.; Zhang, M. T.; Thorp, H.; Meyer, T. J. *J. Am. Chem. Soc.* **2012**, *134*, 18538.
(13) Yuasa, J.; Yamada, S.; Fukuzumi, S. *J. Am. Chem. Soc.* **2008**, *130*, 5808.
(14) Fukuzumi, S.; Kotani, H.; Prokop, K. A.; Goldberg, D. P. *J. Am. Chem. Soc.* **2011**, *133*, 1859.
(15) Yuasa, J.; Fukuzumi, S. *J. Phys. Org. Chem.* **2008**, *21*, 886.
(16) Fukuzumi, S.; Kotani, H.; Lee, Y. M.; Nam, W. *J. Am. Chem. Soc.* **2008**, *130*, 15134.
(17) Matsuo, T.; Mayer, J. M. *Inorg. Chem.* **2005**, *44*, 2150.
(18) Pestovsky, O.; Bakac, A.; Espenson, J. H. *Inorg. Chem.* **1998**, *37*, 1616.
(19) Park, K. K.; Lee, J. H.; Park, J. W. *Bull. Korean Chem. Soc.* **1990**, *11*, 477.
(20) Bakhmutova-Albert, E. V.; Margerum, D. W.; Auer, J. G.; Applegate, B. M. *Inorg. Chem.* **2008**, *47*, 2205.
(21) Park, J.; Morimoto, Y.; Lee, Y. M.; Nam, W.; Fukuzumi, S. *J. Am. Chem. Soc.* **2012**, *134*, 3903.
(22) Jeong, Y. J.; Kang, Y.; Han, A. R.; Lee, Y. M.; Kotani, H.; Fukuzumi, S.; Nam, W. *Angew. Chem., Int. Ed.* **2008**, *47*, 7321.
(23) Ellis, W. W.; Raebiger, J. W.; Curtis, C. J.; Bruno, J. W.; DuBois, D. L. *J. Am. Chem. Soc.* **2004**, *126*, 2738.
(24) Powell, M. F.; Wu, J. C.; Bruice, T. C. *J. Am. Chem. Soc.* **1984**, *106*, 3850.
(25) Anderson, A. G.; Berkelhammer, G. *J. Am. Chem. Soc.* **1958**, *80*, 992.
(26) Segal, R.; Stein, G. *J. Chem. Soc.* **1960**, 5254.
(27) Johnston, C. C.; Gardner, J. L.; Suelter, C. H.; Metzler, D. E. *Biochemistry* **1963**, *2*, 689.
(28) Vaneikeren, P.; Grier, D. L.; Eliason, J. *J. Am. Chem. Soc.* **1979**, *101*, 7406.
(29) Values for $pK_a(NADH^{\bullet+}) = -3.5$ and $E^{\circ\prime}$ for the $NADH/NADH^{\bullet+}$ and $NAD^{\bullet}/NAD^{+}$ couples were taken from reference Carlson, B. W.; Miller, L. L.; Neta, P.; Grodkowski, J. *J. Am. Chem. Soc.* **1984**, *106*, 7233.
(30) $E^{\circ\prime}$ values for the $BNAH/BNA^{\bullet+}$ and $BNA^{\bullet}/BNA^{+}$ couples were taken from reference Zhu, X. Q.; Zhang, M. T.; Yu, A.; Wang, C. H.; Cheng, J. P. *J. Am. Chem. Soc.* **2008**, *130*, 2501 in acetonitrile (the values were obtained by Osteryoung square wave voltammetry measurements, 0.6 V vs NHE was used for correction of ferrocene couple) with the pK_a for $BNAH^{\bullet+}$ assumed to be the same as the pK_a for $NADH^{\bullet+}$.
(31) Hamann, T. W.; Gstrein, F.; Brunschwig, B. S.; Lewis, N. S. *J. Am. Chem. Soc.* **2005**, *127*, 7815.
(32) Caughey, W. S.; Schellenberg, K. A. *J. Org. Chem.* **1966**, *31*, 1978.
(33) Paabo, M.; Bates, R. G. *J. Phys. Chem.* **1970**, *74*, 706.
(34) Covington, A. K.; Paabo, M.; Robinson, R. A.; Bates, R. G. *Anal. Chem.* **1968**, *40*, 700.
(35) All KIEs in this work were determined from the ratios of rate constants when employing *N*-benzyl-1,4-dihydronicotinamide and the corresponding dideuterated compound, including both the primary and secondary kinetic isotope effects.
(36) Yuasa, J.; Yamada, S.; Fukuzumi, S. *Angew. Chem., Int. Ed.* **2008**, *47*, 1068.
(37) Including solvent and substrate kinetic isotope effects.
(38) Ess, D. H.; Schauer, C. K.; Meyer, T. J. *J. Am. Chem. Soc.* **2010**, *132*, 16318.
(39) Coleman, C. A.; Rose, J. G.; Murray, C. J. *J. Am. Chem. Soc.* **1992**, *114*, 9755.
(40) Murray, C. J.; Webb, T. *J. Am. Chem. Soc.* **1991**, *113*, 7426.
(41) Fukuzumi, S.; Ishikawa, M.; Tanaka, T. *J. Chem. Soc., Perkin Trans. 2* **1989**, 1811.
(42) Clark, J.; Bakavoli, M. *J. Chem. Soc., Perkin Trans. 1* **1977**, 1966.
(43) The rate constant for deprotonation of $BNAH^{\bullet+}$ is assumed to be close to $3.5 \times 10^6\ s^{-1}$, which was reported for $NADH^{\bullet+}$ in reference Zielonka, J.; Marcinek, A.; Adamus, J.; Gebicki, J. *J. Phys. Chem. A* **2003**, *107*, 9860.